International Journal of Microscale and Nanoscale Thermal … ISSN: 1949-4955
Volume 4, Number 3/4

EFFECT OF ASPECT RATIO OF RECTANGULAR MICROCHANNELS ON THE AXIAL BACK CONDUCTION IN ITS SOLID SUBSTRATE

***Manoj Kumar Moharana*[*,1] *and Sameer Khandekar*[2#]**
[1]Department of Mechanical Engineering
National Institute of Technology Rourkela, Rourkela, Odisha, India
[2]Department of Mechanical Engineering
Indian Institute of Technology Kanpur, Kanpur, UP, India

ABSTRACT

Microchannels machined on flat solid substrates (metallic/non-metallic) are widely used in many engineering heat transfer applications. Such applications, on most occasions, involve conjugate effects, overlooking of which often leads to misinterpretation of transfer coefficients. In this background, a conjugate three-dimensional numerical simulation of simultaneously developing laminar flow in rectangular microchannels is reported to quantify the effect of channel aspect ratio on axial back conduction in the substrate, which eventually affects the heat transfer coefficient. A substrate of fixed size (0.6 mm × 0.4 mm × 60 mm) is considered while the channel width and height are independently varied such that the channel aspect ratio (width/height) varies from 0.45 to 4.0. Considering the fact that axial conduction dominates at low flow rates, the flow Reynolds number is kept constant at 100. The thermal conductivity of the solid substrate as well as the working fluid are considered in the conjugate formulation. Constant heat flux is applied at the bottom of the substrate while all its other surfaces are kept insulated. To understand the effect of channel aspect ratio on axial back conduction, this ratio is varied in four different ways so as to maintain a constant (i) area of channel cross-section, (ii) heating perimeter, (iii) channel width, and (iv) channel height. It is found that there exists an optimum value of conductivity ratio of solid to fluid, at which the average Nusselt number over the channel length is maximum. For a given flow configuration, the local and the average Nusselt number over the total channel length is found to be function of channel aspect ratio, with a minimum in the Nusselt number always observable. This minimum value corresponds to an aspect ratio of approximately two or slightly less than two, depending on the way channel aspect ratio is varied. As a result of this conjugate heat transfer behaviour, two channels having different channel aspect ratios can have same thermal performance in terms of average Nusselt number.

[*] Corresponding author: moharanam@nitrkl.ac.in; Tel: +91-661-246-2533, Fax: +91-661-247-2926.
[#] samkhan@iitk.ac.in; Tel: +91-512-259-7038, Fax: +91-512-259-7408.

Keywords: Simultaneously developing flow, Rectangular microchannels, Aspect ratio, Conjugate heat transfer, Axial heat conduction, Optimum Nusselt number

NOMENCLATURE

A_f	cross-sectional area of channel i.e. fluid, m^2
A_s	cross-sectional area of solid substrate, m^2
A_{sf}	ratio of A_s and A_f (-)
C_p	specific heat, J/kg-K
D_h	hydraulic diameter, m
h	heat transfer coefficient, W/m^2-K
H	thickness of the substrate, m
k_f	thermal conductivity of working fluid, W/m-K
k_s	thermal conductivity of solid substrate, W/m-K
k_{sf}	ratio of k_s and k_f (-)
k_{sf}^*	value of k_{sf} at which $\overline{Nu}$ is maximum for any channel size (-)
L	length of the channel, m
Nu	Nusselt number (hD_h/k_f)
$\overline{Nu}$	average Nusselt number over the channel length (-)
P_h	heating perimeter, m
Pr	Prandtl number ($C_p\mu/k_f$)
Q	total heat applied at the bottom of the substrate, W
$\overline{q}'$	average heat flux experienced at the channel walls, W/m^2
$\overline{q}'_{applied}$	heat flux applied at the bottom of the substrate, W/m^2
Re	Reynolds number ($\rho u D_h/\mu$)
T	temperature, K
$\overline{T}$	average temperature, K
W	width of the substrate, m
z	axial coordinate, m
z^*	non-dimensional axial distance along channel length (-)

Greek symbols

δ	thickness, m
δ_f	height of the channel, m
δ_s	thickness of the solid substrate below the channel, m
δ_{sf}	ratio of δ_s and δ_f (-)
ε	channel aspect ratio (ω_f/δ_f) (-)
ω	width, m
ω_f	channel width, m
ω_s	width of channel vertical wall, m
μ	dynamic viscosity, Pa-s
ρ	density, kg/m^3

ϕ	non-dimensional local heat flux (-)
Θ	non-dimensional temperature (-)

Subscripts

f	fluid
i	inlet condition
o	outlet condition
s	solid
w	wall surface
z	axial length along the channel

1. INTRODUCTION

In conventional sized duct/channels, under fully developed flow conditions, a constant heat flux boundary condition at the solid-fluid interface leads to maximum heat transfer coefficient. In many engineering applications a situation with constant heat flux on one, or some of the surfaces being heated, arises. While the objective ought to be to have the constant heat flux exactly at the solid-fluid interface, in reality, for several practical limitations, the surface on which the constant heat flux is actually applied is at a certain finite distance from the true solid-fluid interface. This leads to multi-dimensional conjugate heat transfer, depending on several factors, viz., the geometric configuration of the solid and fluid domain, thermo-physical properties of the solid substrate and fluid involved, and flow conditions. In some cases it is likely that the effective thermal resistance in the solid medium in the axial direction is such that heat actually flows by conduction in the solid substrate in the axial direction, opposite to the streamwise direction. This phenomena of 'axial back conduction', distorts the true boundary condition of constant heat flux at the solid-fluid interface. This, in turn, reduces heat transfer coefficient. The effect of axial conduction gets magnified in microchannel systems and likely to give inaccurate heat transfer coefficient estimation, if over-looked.

The study of axial conduction in the solid domain in a convective heat transport system was carried out as early as in 1964, by Bahnke and Howard [1]. Later on Petukhov [2] studied axial conduction in the solid wall of a circular tube using a parameter which is function of thermal conductivity ratio of the solid walls and the working fluid, and the tube thickness to inner radius ratio. Other similar studies were done by Faghri and Sparrow [3], Chiou et al. [4], and Cotton and Jackson [5]. Though the study on axial conduction continued with time, the numbers of studies are quiet few. The study on axial conduction again gained momentum with development of microscale heat transfer devices. This is because of relative importance of axial conduction effect in such small geometries, as compared to heat transfer applications employing conventional sized channels. Peterson [6] numerically studied conduction effects in microscale counter flow heat exchangers. Maranzana et al. [7] introduced a number called axial conduction number (M) which is defined as the ratio of the conductive heat flux to the convective counterpart. Maranzana et al. [7] also stated that axial conduction in the solid substrate will be negligible if $M < 0.01$. Li et al. [8] and Zhang et al. [9], based on their study on conjugate heat transfer in thick circular tubes concluded that the criterion for neglecting

axial conduction as proposed by Maranzana et al. [7] may not be always valid. They stated that depending on the boundary conditions and geometrical parameters the criteria for judging the effect of axial wall conduction may vary on a case-to-case basis.

Moharana et al. [10] numerically investigated the exactness of the constant heat flux boundary condition at the channel solid-fluid interface. Based on the experimental study and numerical investigation, they found that due to axial back conduction, conjugate effects become prominent and the experimental heat transfer data, especially at lower Re is affected, leading to lower estimation of experimental local Nusselt number. They also found that, all other parameters remaining identical, substrates with lower conductivity reduce effects of axial back conduction. Karakaya and Avci [11] simulated coupled methane oxidation/iso-octane steam reforming in parallel microchannels and found the effect of axial conduction in the microreactor substrate on its axial temperature distribution and hydrogen yield. They found that iron serves as the best wall material on the basis of highest hydrogen yield, compared to steel and alumina. Chein et al. [12] numerically studied effects of reformer wall axial conduction on performance of methanol steam reforming. They suggested that the methanol steam reformer with low wall thermal conductivity and thin wall thickness have a small axial conduction parameter and results in higher performance.

Recently, Moharana et al. [13] presented a detailed review of axial conduction and carried out numerical analysis of axial conduction in a circular micro tube and a square shaped microchannel on a solid substrate, considering wide parametric variations. Their study suggests that for both the microtube as well as square microchannel on solid substrate, there exists an optimum value of conductivity ratio (conductivity of the solid substrate material to conductivity of working fluid) which maximizes the average Nusselt number over the channel length. This observation was based on an extensive parametric variation of conductivity ratio, flow Re and substrate thickness, while the heating perimeter was kept constant i.e. a square channel of constant dimensions. This can be explained as follows: Higher conductivity ratio leads to severe axial back conduction, thus decreases average Nu. Very low value of conductivity ratio leads to a situation which is qualitatively similar to the case of zero thickness substrate with constant heat flux applied on one wall only (the other three sides being adiabatic). This again lowers the average value of Nu. A very close observation to understand this phenomenon revealed that with decreasing conductivity ratio, the thermal resistance to flow of heat to the two vertical walls of the square channel increases. From this observation it is expected that, all other factors remaining the same, the channel aspect ratio will also play a major role in the conjugate heat transfer process.

In this background, we have conducted a three-dimensional numerical investigation, using commercially available Ansys-Fluent®, to understand and highlight the effect of channel aspect ratio (ratio of channel width to the channel height) on the axial wall conduction in a steady-state laminar incompressible simultaneously developing flow and ensuing heat transfer in rectangular microchannels. Considering extensive use of rectangular microchannels for a variety of practical applications, we consider the system as shown schematically in Figure 1. A uniform wall heat flux applied at the bottom of the substrate with all other surfaces being insulated is modelled, as shown. Thermophysical properties of both the solid and the fluid domain are assumed to be constant. Peripherally averaged (over three heating sides) local heat flux, wall temperature and average bulk fluid temperature are numerically calculated as functions of the dimensionless axial distance, channel aspect ratio, and thermal conductivity ratio of solid to fluid. Simulations have been carried out for a wide

range of substrate wall to fluid conductivity ratio (12.2 - 635) and channel aspect ratio (0.45 - 4.0) for a fixed substrate dimension. A low flow rate case (Re = 100) has been reported here, as it represents a typical case, prone to the effects of axial conduction [13]. These parametric variations cover the typical range of applications encountered in micro-fluids/micro-scale heat transfer domains. To discern the explicit effect of channel aspect ratio and the heating perimeter, four types of channel aspect ratio variation, for a fixed size substrate, are considered. The channel aspect ratio is varied so as to maintain a constant (i) area of channel cross-section, (ii) heating perimeter, (iii) channel width, and (iv) channel height. Peripherally averaged local heat flux, wall temperature and average bulk fluid temperature are numerically calculated as functions of the dimensionless axial distance, channel aspect ratio, and thermal conductivity ratio of solid to fluid. Extensive grid independence and validation of the numerical scheme is done before carrying out the simulations reported here.

2. NUMERICAL ANALYSIS

In the present investigation it is assumed that the heat transfer and fluid flow takes place at steady state, the flow is laminar, incompressible with constant thermo-physical properties and the amount of heat loss either by radiation or by means of natural convection is negligible.

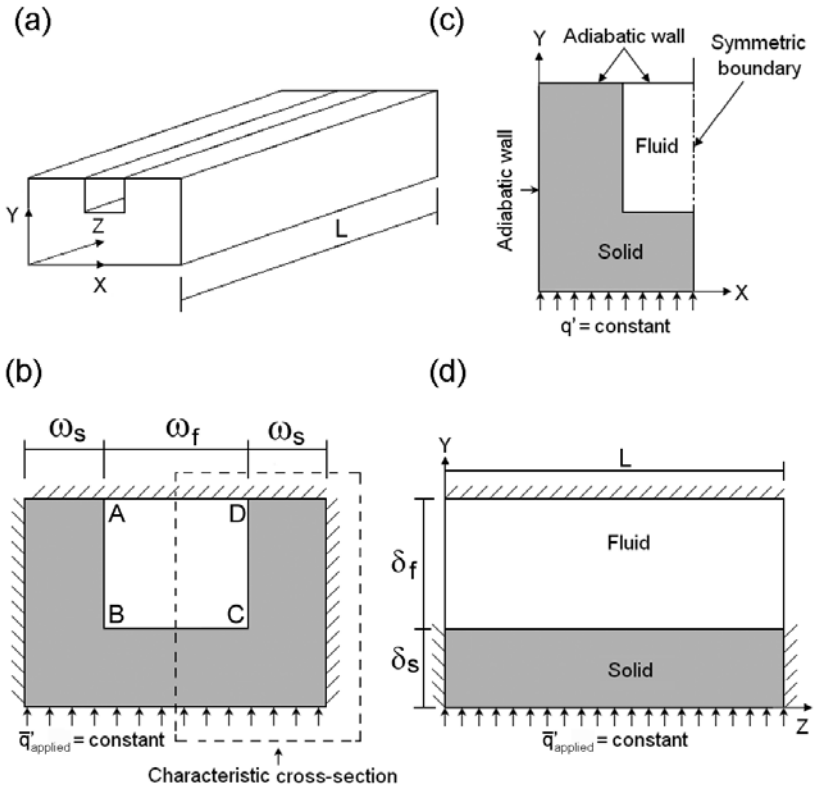

Figure 1. Schematic of (a) Microchannel with conductive wall (b) Channel cross section (c) Computational domain (d) Transverse sectional view along the plane of symmetry.

Again referring to Figure 1, the width ($2\cdot\omega_s+\omega_f$), the thickness ($\delta_s+\delta_f$), and the length (L) of the substrate are kept constant in the computational model at 0.6 mm, 0.4 mm, and 60 mm respectively. The aspect ratio of the channel in which the fluid is flowing is varied, i.e., by varying the channel width (ω_f), and the channel height (δ_f); thus, the hydraulic diameter (D_h) of the channel ranges from 0.16 - 0.203 mm**.** In actual computations, only one half of this section (see Figure 1 (c)), along the vertical plane of symmetry, was considered. As discussed earlier, a constant heat flux boundary condition is applied at bottom of the substrate, and all other outer surfaces are insulated, as shown in Figure 1. Coupled equations for conservation of mass, momentum and energy are solved on this domain using commercial platform Ansys-Fluent®. The multi-grid solution procedure incorporates the 'standard' scheme for pressure discretization and the SIMPLE algorithm for velocity-pressure coupling. Momentum and energy equations are solved using "second order upwind" scheme. Water is used as the working fluid, which enters the microchannel with a uniform 1-D velocity profile, at an inlet temperature of 300K. Thus, the flow is hydrodynamically as well as thermally developing in nature during its transit in the channel.

The computational domain was meshed using hexahedral elements and the grid independence was ensured before deciding the grid size for each case under consideration. For example, local Nusselt number calculated for a substrate with $\delta_{sf} = 1$ (δ_{sf} is defined as the ratio of δ_s and δ_f , where δ_s is the thickness of the solid substrate below the channel, and δ_f is defined as the height of the channel (see Figure 1)) for three mesh sizes of 45×60×150, 60×80×200 and 75×100×250 (for half of the geometry as shown in Figure 1), for Re = 100, is as shown in Figure 2.

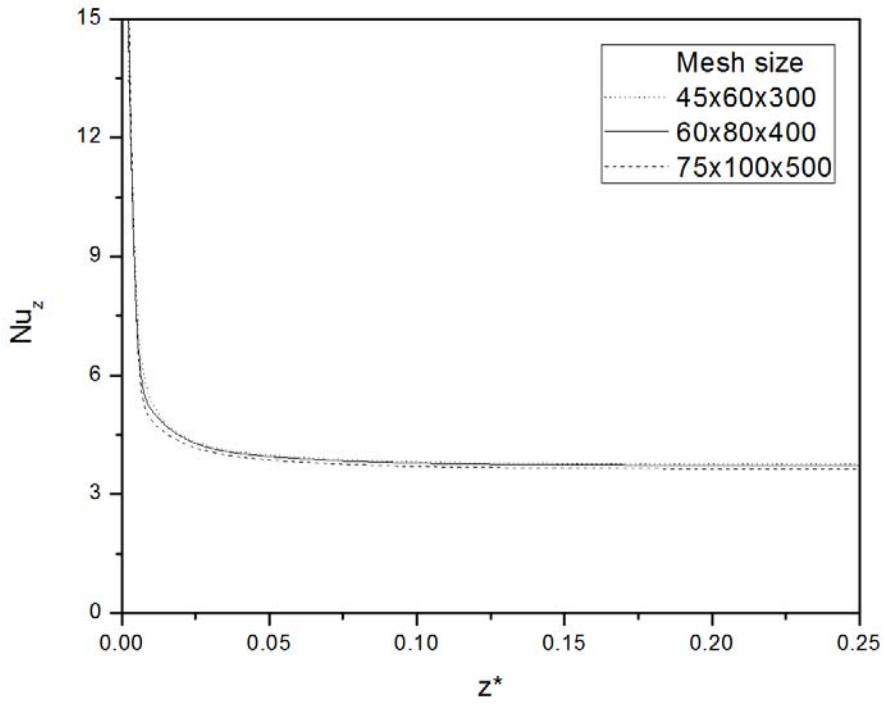

Figure 2. Variation of local Nusselt number along the streamwise direction for a channel of size 0.4 mm × 0.4 mm × 60 mm, with $\delta_{sf} = 1$.

The peripheral averaged local Nusselt number at the fully developed flow regime near the channel outlet changed by 1.06% from the mesh size of 45×60×150 to 60×80×200, and changed by less than 1% on further refinement to mesh size of 75×100×250. As we moved from first to the third mesh, no appreciable change is observed. So, the intermediate grid (60×80×200) was selected, which corresponds to actual physical average spacing of 0.01 mm along the width and height (x and y axis) and 0.3 mm along the channel length (z axis). Finer meshing was used in the channel entrance and the boundary layers.

3. DATA REDUCTION

The microchannel hydraulic diameter (D_h), channel aspect ratio (ε), conductivity ratio (k_{sf}), cross sectional area ratio (A_{sf}) are defined (with reference to Figure 1) as follows:

$$A_f = \omega_f \cdot \delta_f, \;\; A_s = (\omega_f + 2\omega_s)(\delta_s + \delta_f) - A_f \tag{1}$$

$$D_h = \frac{2A_f}{\delta_f + \omega_f}, \;\; \varepsilon = \frac{\omega_f}{\delta_f}, \;\; k_{sf} = \frac{k_s}{k_f}, \;\; A_{sf} = \frac{A_s}{A_f} \tag{2}$$

where ω_f = channel width, δ_f = channel height, ω_s = width of channel vertical wall, δ_s = thickness of channel horizontal wall i.e. substrate thickness below channel bottom wall, k_s = thermal conductivity of the solid substrate, k_f = thermal conductivity of the working fluid, A_s = Area of cross section of the solid substrate, A_f = area of cross section of channel. The heating perimeter (P_h) is defined as the perimeter of the conjugate walls of the channel, is represented as

$$P_h = \omega_f + 2\delta_f \tag{3}$$

The axial coordinate, z, is non-dimensionalized as:

$$z^* = z / L \tag{4}$$

where L = length of the channel. The applied heat flux at the bottom of the substrate is defined as follows:

$$\overline{q}'_{applied} = \frac{Q}{\left(2 \cdot \omega_s + \omega_f\right) L} \tag{5}$$

where, Q is the heat input to the bottom of the substrate. The ideal heat flux at the solid fluid interface is given by:

$$\overline{q}' = \overline{q}'_{applied} \frac{\left(2 \cdot \omega_s + \omega_f\right)}{\left(2 \cdot \delta_f + \omega_f\right)} \tag{6}$$

The non-dimensional local heat flux at the fluid-solid interface is given by:

$$\phi = q'_z / \overline{q}' \tag{7}$$

where q'_z is the peripheral averaged local heat flux transferred at the solid-fluid interface along the channel length (only the three heating sides are included for calculating this peripheral average value, as the top wall is adiabatic). The dimensionless bulk fluid and channel wall temperatures are given by:

$$\Theta_f = \frac{\overline{T}_f - \overline{T}_{fi}}{\overline{T}_{fo} - \overline{T}_{fi}} \tag{8}$$

$$\Theta_w = \frac{\overline{T}_w - \overline{T}_{fi}}{\overline{T}_{fo} - \overline{T}_{fi}} \tag{9}$$

where $\overline{T}_{fi}$ and $\overline{T}_{fo}$ are the average bulk fluid temperature at the channel inlet and outlet respectively; $\overline{T}_f$ is the average bulk fluid temperature at any location and $\overline{T}_w$ is the peripheral average wall temperature at the same location (here too, only three heating sides are included to calculate the peripheral average wall temperature). The local Nusselt number is then given by:

$$Nu_z = h_z \cdot D_h / k_f \tag{10}$$

where the local heat transfer coefficient is given by:

$$h_z = \frac{q'_z}{\left(\overline{T}_w - \overline{T}_f\right)} \tag{11}$$

The average Nusselt number over the whole channel length is given by:

$$\overline{Nu} = \int_{z=0}^{L} Nu_z dz \tag{12}$$

4. RESULTS AND DISCUSSION

As stated earlier, the recent study on axial conduction [13] indicated that, all other factors remaining the same, the channel aspect ratio is likely to play a major role in the conjugate heat transfer process. Therefore the width (W), thickness (H), and length (L) of the substrate in the computational model are kept constant at 0.6 mm, 0.4 mm, and 60 mm, respectively as shown in Figure 3.

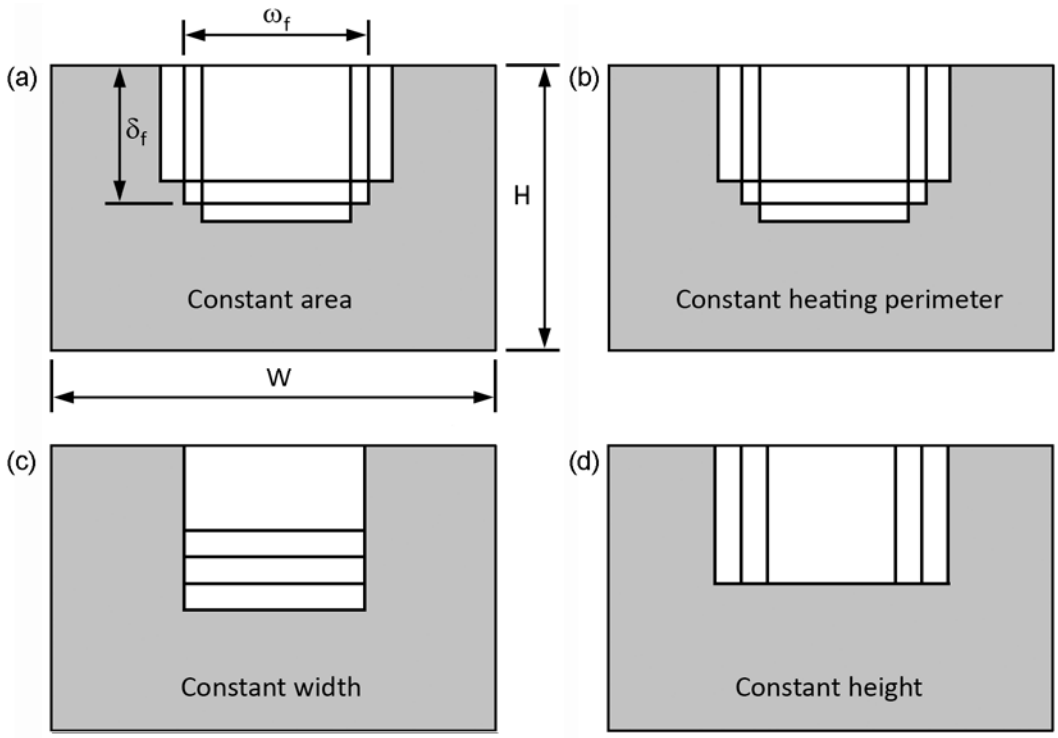

Figure 3. For a fixed substrate size, the microchannel aspect ratio are varied by maintaining constant (a) area of cross section ($\omega_f \cdot \delta_f$) of microchannel (b) heating perimeter (P_h) (c) channel width (ω_f), and (d) channel height (δ_f).

While the length (L) of the channel is kept constant at 60 mm, the width (ω_f) and the height (δ_f) of the channel are varied to understand the effect of the channel aspect ratio (ε) on the conjugate heat transfer behaviour. This is because, as the aspect ratio of the channel varies, the heating perimeter (P_h), hydraulic diameter (D_h), area of cross section ratio (A_{sf}) etc. also varies. This makes the conjugate system more complicated. Table 1 collates the full range of parametric variation considered in the present study. In all cases Re = 100 is chosen, considering that the lower the flow Re, the more prone it is to axial back conduction [13]. With increasing Re, the effect of axial back conduction decreases, thus there is increase in magnitude of both average and local Nu.

Table 1. Range of parameters considered for simulations

Re	k_{sf}	ε	Pr
100	12.2 - 635.0	0.45 - 4.0	5.85

To discern the explicit effect of channel aspect ratio, the channel width and height are varied such that the area of cross-section of the channel remains constant (see Figure 3(a)). Since the substrate size is also constant, the ratio of area of cross section of solid substrate to the channel (A_{sf}) is constant and equal to 5.0. For each channel size, simulations have been performed for $k_{sf} \sim 12.2 - 635$. The working fluid used for all cases is water at inlet temperature of 300 K. Heat flux is applied on the bottom surface of the substrate which lies at

a certain finite distance from the channel walls. Moreover, of the three conjugate walls of the channel, the channel bottom wall is parallel to the substrate bottom surface on which constant heat flux is applied, and the remaining two walls are perpendicular to the substrate bottom surface. The main parameters of interest are (a) peripheral average local heat flux (b) local bulk fluid temperature (c) peripheral average local wall temperature. These parameters allow us to determine the extent of axial conduction on the local Nu.

To find the magnitude of heat flux experienced at the conjugate walls of the rectangular channel, the axial variation of dimensionless heat flux, ϕ at the solid-fluid interface is presented in Figure 4.

At very low conductivity ratio k_{sf} (≈ 12.2), the actual heat flux experienced at the solid-fluid interface is approximately constant along the channel length. This can be observed in Figure 4 (a). At higher value of k_{sf} (≈ 635), the heat flux experienced along the length of the channel substantially deviates from the ideal value of 1.0, especially at the inlet and the outlet region of the channel.

Next, the axial variation of bulk fluid and channel wall temperature are explored, which are shown in Figure 5. Ideally, the fluid and the wall temperature varies linearly in the fully developed region. This trend is followed at lower k_{sf} (≈ 12.2), which can be seen in Figure 5 (a). At higher k_{sf} (≈ 635), the fluid and the wall temperature are deviating from linearity towards the end of the channel (see Figure 5 (c)). Secondly, the wall temperature at any axial location of the channel is found to be varying with channel aspect ratio irrespective of the value of k_{sf}, and the value of wall temperature is maximum when channel aspect ratio $\varepsilon = 2.0$. The bulk fluid temperature is independent of channel aspect ratio, ε.

The axial variation of (a) heat flux at the solid-fluid interface, and (b) wall and bulk fluid temperatures will influence the behavior of the local Nusselt number along the channel length, as shown in Figure 6. Conventionally, the Nusselt number in the fully developed region is constant. This trend is followed at lower k_{sf} (≈ 12.2), which can be seen in Figure 6 (a). At higher k_{sf} (≈ 635), the Nusselt number does not remain constant towards the end of the channel (see Figure 6 (c)). Rahimi and Mehryar [14] had also reported similar phenomena where they found that the axial heat conduction in the microchannel wall decreases the local Nusselt number at the far downstream regions of the microchannel. Secondly, the Nusselt number at any axial location of the channel (Nu_z) is found to be varying with channel aspect ratio irrespective of the value of k_{sf}, and the value of Nu_z at any location except near the entrance is found to be minimum when the channel aspect ratio $\varepsilon = 2.0$.

From Figure 6, it is logically expected that the average Nusselt number ($\overline{Nu}$) over the whole channel length will also be minimum, corresponding to $\varepsilon = 2.0$, while the other parameters i.e., Re and k_{sf} are constant. The variation of average Nusselt number ($\overline{Nu}$) over the whole channel length is plotted as function of conductivity ratio, k_{sf} as the channel aspect ratio ε is varied. This is shown in Figure 7 (a). First, the occurrence of the optimum k_{sf} for maximizing the average Nusselt number is seen in Figure 7 (a) for every channel aspect ratio considered; this is inline with the previous study by Moharana et al. [13]. The prominent observation is that the magnitude of is strong function of channel aspect ratio and is minimum at channel aspect ratio $\varepsilon = 2.0$. increases with both increasing as well as decreasing channel aspect ratio away from $\varepsilon = 2.0$.

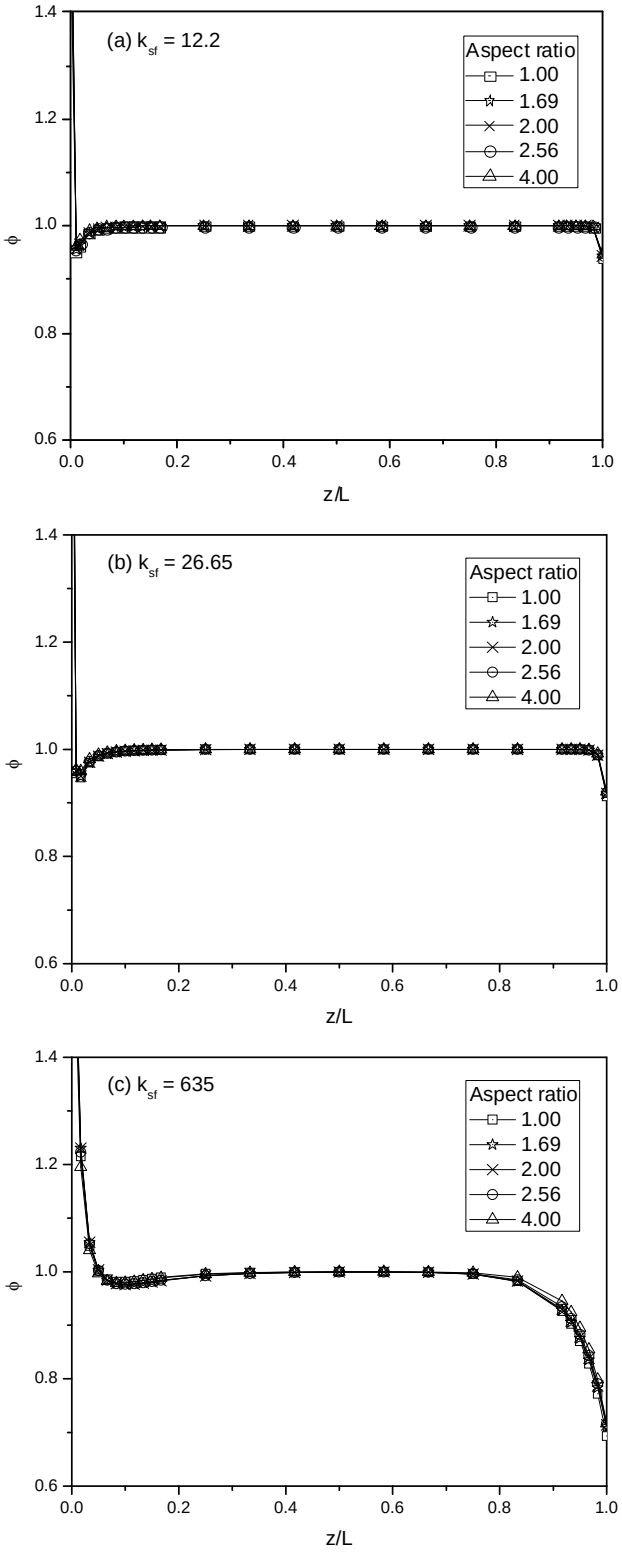

Figure 4. Variation of dimensionless local surface heat flux along the channel length.

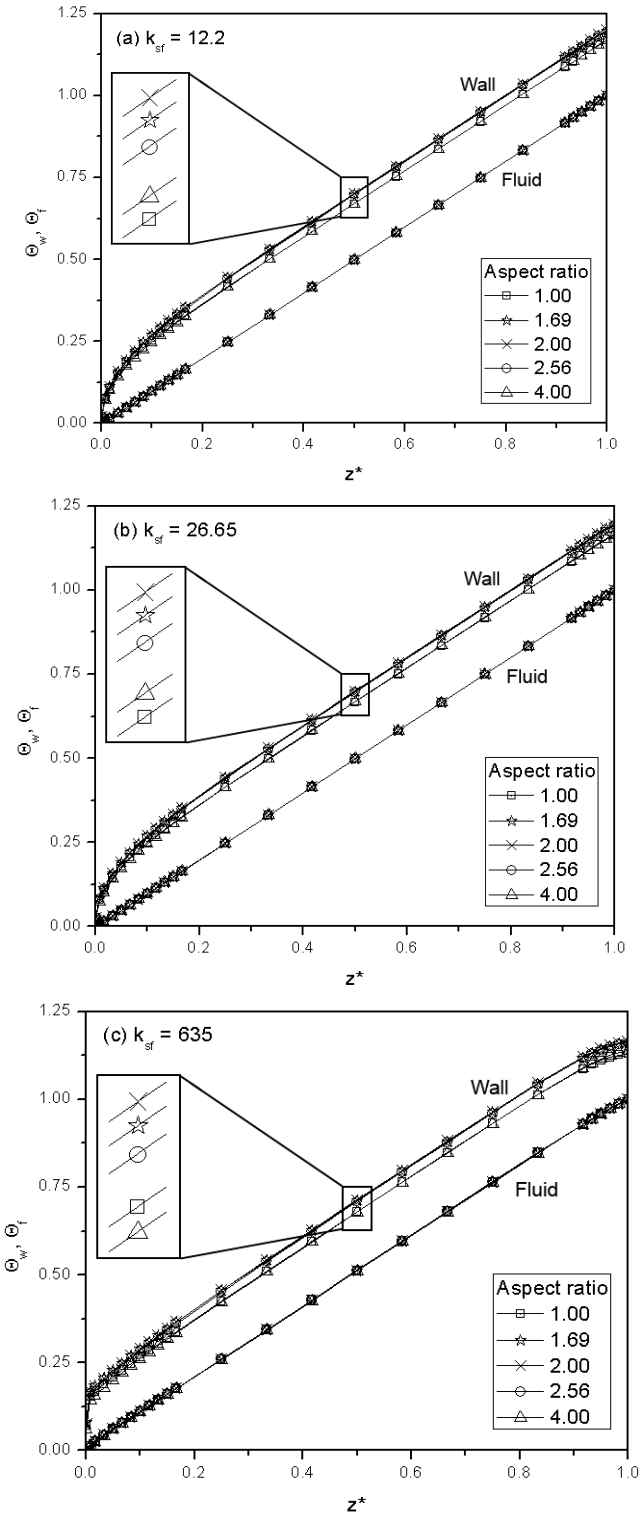

Figure 5. Variation of dimensionless local wall and local bulk fluid temperature along the channel length.

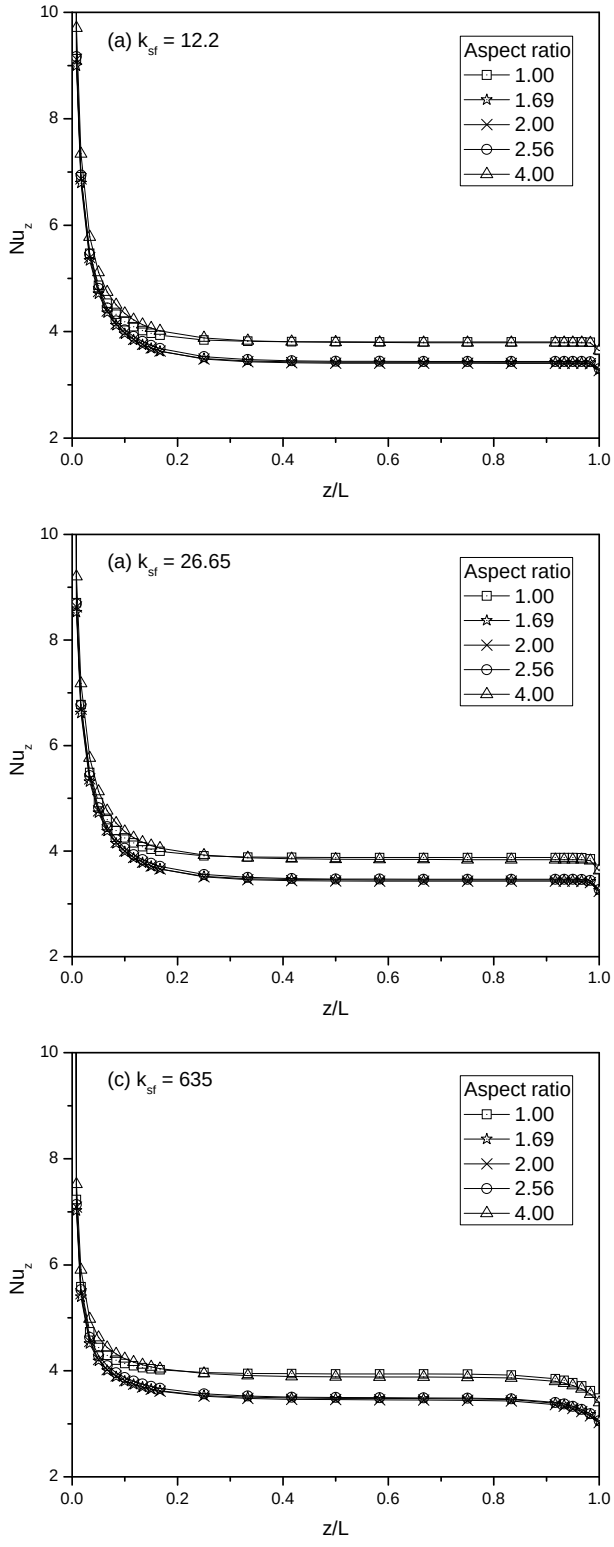

Figure 6. Variation of local Nusselt Number along the channel length.

From the above discussion it is clear that the channel aspect ratio play an important role in the heat transfer process, in addition to other parameters such as Re, k_{sf}, and substrate size. As discussed earlier, Moharana et al. [13] had numerically studied effect of Re, k_{sf}, and substrate size on axial conduction; the present work is focused on role of channel aspect ratio. With varying channel height and width (i.e. channel aspect ratio) while area of cross section of the channel (A_f) is constant, the channel heating perimeter (P_h) is varying. For this kind of variation in channel dimensions, the channel aspect ratio $\varepsilon = 2.0$ corresponds to minimum heating perimeter P_h. From this information now it may be concluded that minimum heating perimeter at $\varepsilon = 2.0$ leads to minimum Nu_z and subsequently minimum $\overline{Nu}$, as observed in Figure 6 and Figure 7 (a), respectively.

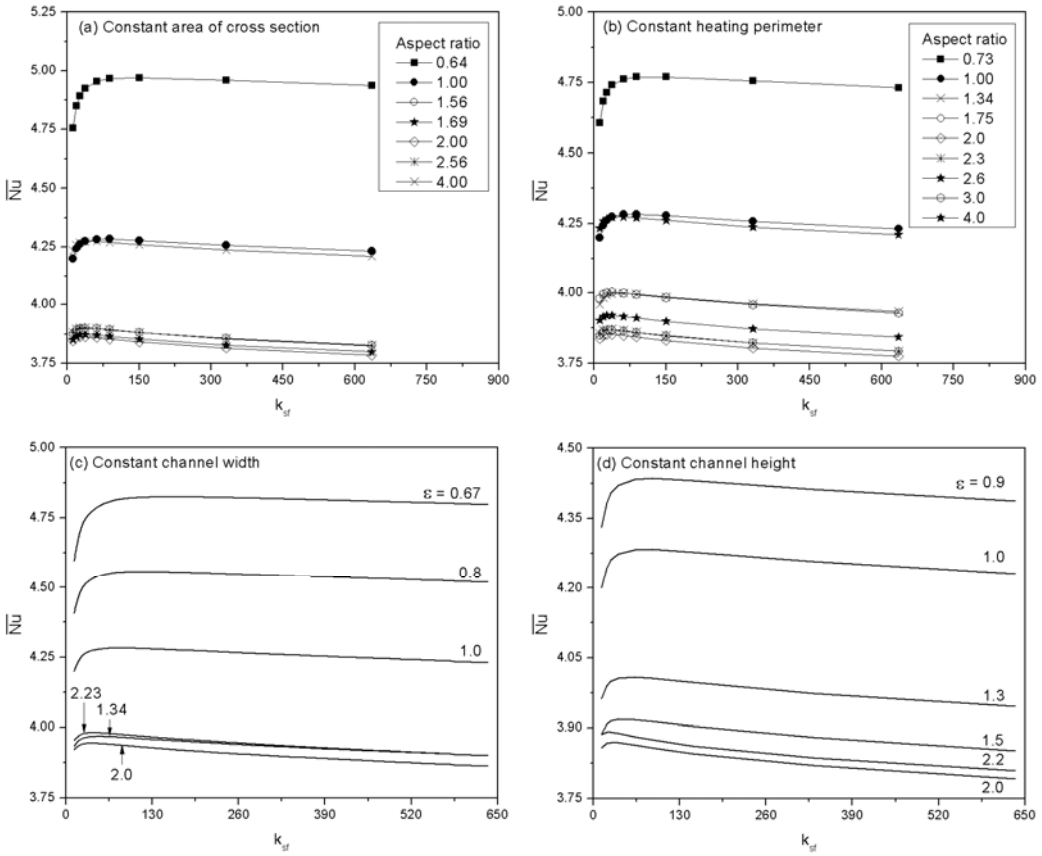

Figure 7. Variation of average Nusselt number of the rectangular microchannel with varying channel aspect ratio as a function of conductivity ratio (k_{sf}) for (a) constant area of channel cross section (b) constant heating perimeter (c) constant channel width (d) constant channel height.

At this stage, it becomes important to understand the effect of heating perimeter. In this background, the channel aspect ratio is again varied such that the heating perimeter (P_h) of the channel is constant (see Figure 3(b)). Here, it may be expected that the channel aspect ratio will not influence the value of Nu_z and $\overline{Nu}$, as P_h is constant. So, the variation of $\overline{Nu}$ is now plotted as function of k_{sf} for varying channel aspect ratio ε while the heating perimeter (P_h) is maintained constant. This is shown in Figure 7 (b). Here too the occurrence of the optimum

k_{sf} for maximizing $\overline{Nu}$ is seen. But, most significantly, contrary to the earlier observation that for constant heating perimeter, channel aspect ratio will not influence the value of $\overline{Nu}$, it is found that the magnitude of $\overline{Nu}$ is a strong function of channel aspect ratio and is again minimum corresponding to channel $\varepsilon = 2.0$.

Therefore, to understand the effect of channel aspect ratio on axial back conduction more clearly, the aspect ratio of the channels is again varied in two more ways such that (i) channel width is maintained constant (ii) channel height is kept constant, as shown in Figure 3 (c-d). The variation of $\overline{Nu}$, as a function of k_{sf} for different channel aspect ratio ε are plotted in Figure 7 (c) and (d) respectively for constant channel width and channel height. This makes a total of four ways for the parametric variation of channel aspect ratio, i.e. maintaining constant (i) area of cross-section of the channel (ii) heating perimeter of the channel (iii) channel width (iv) channel height. In Figure 7 (c-d) also it is observed that the magnitude of $\overline{Nu}$ is again minimum corresponding to $\varepsilon = 2.0$.

Figure 8 shows the value of k_{sf} at which $\overline{Nu}$ is maximum (in Figure 7) at different channel aspect ratios, denoted by k_{sf}^{*}. It shows that as the aspect ratio increases, the k_{sf} value at which $\overline{Nu}$ is maximum (i.e., k_{sf}^{*}) rapidly goes down. However, with increasing the channel aspect ratio further, the value of k_{sf}^{*} again increases marginally. This trend is followed by all the four cases, as shown.

To understand the effect of channel aspect ratio more clearly than what is observed in Figure 7, the variation of $\overline{Nu}$, as a function of channel aspect ratio, at constant k_{sf} ($k_{sf} = 635$, 12.19 and k_{sf}^{*} (as shown in Figure 8)) are shown in Figure 9. Figure 9 (a-d) corresponds to Figure 7 (a-d) representing constant (i) area of channel cross section, (ii) heating perimeter (iii) channel width, and (iv) channel height, respectively. In Figure 9 (a), it can be observed that the magnitude of $\overline{Nu}$ is minimum at channel aspect ratio $\varepsilon = 2.0$, which corresponds to minimum heating perimeter, i.e., $(2\cdot \delta_f + \omega_f)$ = minimum. For $\varepsilon < 2.0$, as aspect ratio decreases $\overline{Nu}$ increases. Again for $\varepsilon > 2.0$, as aspect ratio increases $\overline{Nu}$ increases. At this point it seems the least heating perimeter at $\varepsilon = 2.0$ causes a minima for average Nusselt Number.

In Figure 9 (b) it is also observed that the variation of $\overline{Nu}$ as a function of ε is quite similar to the results presented in Figure 9 (a). In Figure 7 (a) $\overline{Nu}$ varies with channel aspect ratio, so from Fig 7 (a) at first it is apparent that this may be attributed to change in the heating perimeter. However, as seen in Figure 7 (b), in spite of the fact that the heating perimeter is kept constant, average Nusselt number still varies. Thus, from Figure 9 (b) it is clear that the magnitude of $\overline{Nu}$ is independent of heating perimeter of the channel. Figure 9 (c) and Figure 9 (d) presents variation of $\overline{Nu}$ with varying channel aspect ratio while channel width and height are maintained to be constant, respectively. In Figure 9 (c) it is observed that the variation of $\overline{Nu}$ as a function of ε is also similar, as it was in Figure 9 (a) and Figure 9 (b) but the minima is observed at $\varepsilon = 1.8$ instead of at $\varepsilon = 2.0$. Like in Figure 9 (c), the minima in Figure 9 (d) is also observed at $\varepsilon < 2.0$, at $\varepsilon = 1.9$.

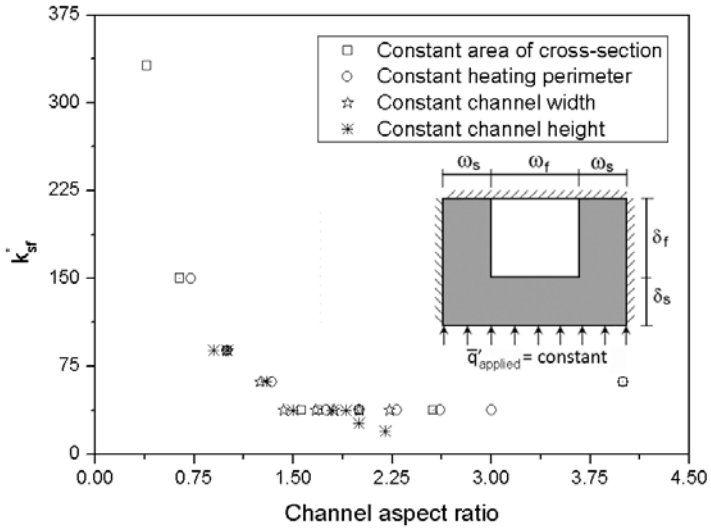

Figure 8. Value of k_{sf} at which $\overline{Nu}$ is maximum at different channel aspect ratios.

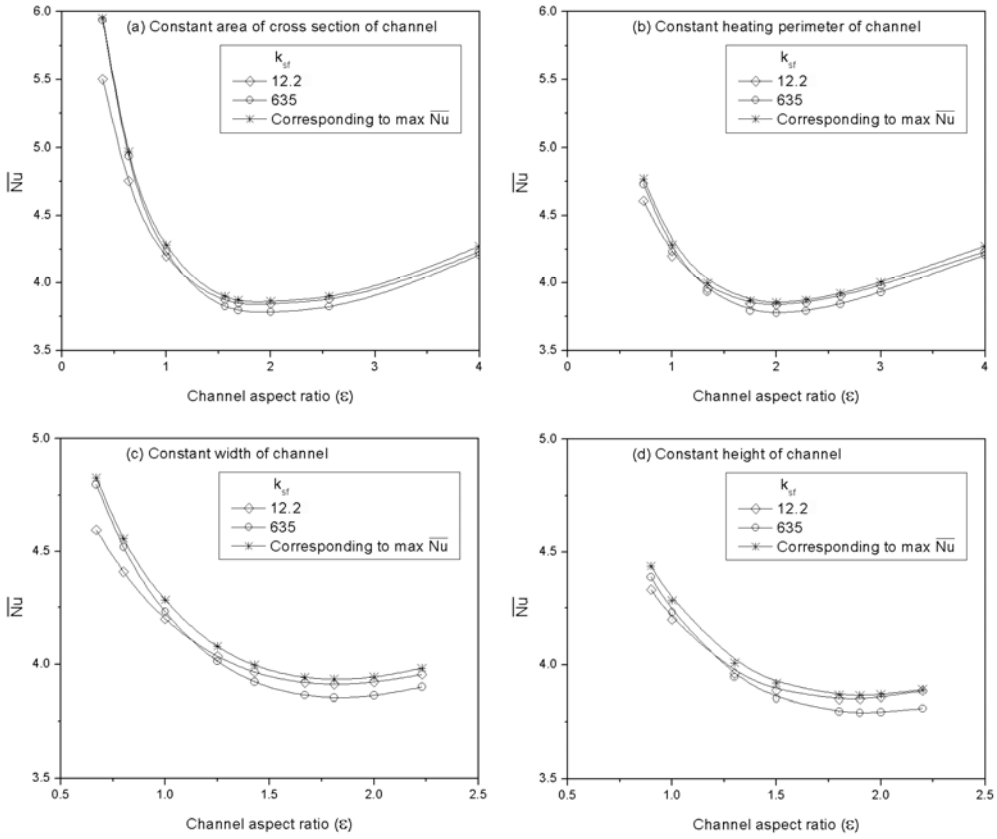

Figure 9. Variation of average Nusselt number of the rectangular microchannel with varying channel aspect ratio at k_{sf} = 635, 12.2 and k_{sf} value at which $\overline{Nu}$ is maximum in each case, as shown in Figure 8.

For all the four cases shown in Figure 9, the rate of increase of $\overline{Nu}$ with decrease in channel aspect ratio is more as compared to increase in channel aspect ratio. This observation is true irrespective of the value of conductivity ratio but the value of conductivity ratio corresponding to peak value of $\overline{Nu}$ is shifting to higher values, with both increasing as well as decreasing channel aspect ratio, i.e., the value of conductivity ratio corresponding to maximum $\overline{Nu}$ is lowest when channel aspect ratio $\varepsilon = 2.0$.

Recently Türkakar and Okutucu-Özyurt [15] studied dimensional optimization of rectangular silicon microchannel heat sinks by minimizing the total thermal resistance. They used four different analytical optimization models based on the work of Liu and Garimella [16], which are valid for uniform heat load condition (without any conjugate effects). Türkakar and Okutucu-Özyurt [15] improved the analytical optimization models by considering the entrance effects and property variations. Their work illustrated that for all the four models used, the thermal resistance decreases with increasing channel height (or decreasing aspect ratio) i.e., optimized geometries have much greater channel heights compared to their channel widths. While this result is certainly in line with the results discussed in Figure 7 and Figure 9, their conclusions are only partly valid; Türkakar and Okutucu-Özyurt [15] did not capture the full spectrum of channel aspect ratios to observe the presence of either maxima or minima. This is because, their domain of findings is limited, based on a single value of k_{sf} and only three values of channel aspect ratios.

From the above discussion it is clear that the channel aspect ratio strongly influences axial back conduction in the substrate and there exists a minimum in the average Nusselt number, approximately near $\varepsilon = 2.0$. Secondly, lower aspect ratio channels result in higher average Nusselt number compared to higher aspect ratio channels, located on the other side of the minimum value. Though decreasing channel aspect ratio or increasing channel height is favourable from a thermal point of view, it is relatively difficult to manufacture low aspect ratio channels compared to high aspect ratio channels. Considering that very high aspect ratio channels are comparatively easy to manufacture and they are also thermally favourable if $\varepsilon > 2.0$, for same thermal performance of two reciprocal valued channel aspect ratios, the channel with higher aspect ratio should be preferred.

SUMMARY AND CONCLUSION

In this work a three-dimensional numerical investigation is reported for flow through a rectangular microchannel on a solid substrate. A substrate of fixed size (0.4 mm × 0.6 mm × 60 mm) with varying channel aspect ratio ($\varepsilon \sim 0.45 – 4.0$) is used to find the effect of aspect ratio on axial back conduction. Heat flux is applied on the bottom surface of the substrate which lies at a certain finite distance from the channel walls. For each channel size, simulations have been performed for $k_{sf} \sim 12.2 – 635$.

The results clearly show that, for a given flow rate and any value of thermal conductivity ratio k_{sf}, a minimum of average Nusselt number occurs with respect to the channel aspect ratio. This minimum corresponds to channel aspect ratio approximately equal to 2.0 or slightly less than 2.0. Decreasing channel aspect ratio beyond this minima value, or increasing channel height for specific channel width, results in the decrease of the effective thermal resistance. Thus, the average Nusselt number increases, irrespective of substrate conductivity.

Only the relative magnitude of average Nusselt number varies with substrate conductivity, as discussed above. Secondly, the effective thermal resistance also decreases with increasing channel aspect ratio for $\varepsilon > 2.0$; thus, the average Nusselt number again increases irrespective of substrate conductivity. But the slope of this rise in average Nusselt number is less compared to the slope when $\varepsilon < 2.0$.

Though decreasing channel aspect ratio or increasing channel height is favourable from thermal point of view, it is relatively difficult to manufacture low aspect ratio channel compared to high aspect ratio channels. Considering that higher aspect ratio channels are comparatively easy to manufacture and they are also thermally favourable if $\varepsilon > 2.0$, for same thermal performance of two different aspect ratio channels, the microchannel with higher aspect ratio should be preferred.

ACKNOWLEDGMENTS

The work is funded by the Department of Science and Technology, Government of India, under the sponsored project No: DST/CHE/20060304 titled 'Micro-devices for Process Applications'.

REFERENCES

[1] G.D. Bahnke, C.P. Howard, The effect of longitudinal heat conduction on periodic-flow heat exchanger performance, *J. Eng. Power* 86 (1964) 105-120.

[2] B.S. Petukhov, Heat transfer and drag of laminar flow of liquid in pipes. *Energiya,* Moscow (1967).

[3] M. Faghri, E.M. Sparrow, Simultaneous wall and fluid axial conduction in laminar pipe-flow heat transfer, *J. Heat Transf.* 102 (1980) 58-63.

[4] J.P. Chiou, The advancement of compact heat exchanger theory considering the effects of longitudinal heat conduction and flow non-uniformity. symposium on compact heat exchangers-history, technological advancement and mechanical design problems. Book no. G00183, HTD Vol. 10, *ASME*, New York (1980).

[5] M.A. Cotton, J.D. Jackson, The effect of heat conduction in a tube wall upon forced convection heat transfer in the thermal entry region. In: *Numerical methods in thermal problems,* vol. (iv), Pineridge Press, Swansea, 504-515 (1985).

[6] R.B. Peterson, Numerical modeling of conduction effects in microscale counter flow heat exchangers, *Microscale Thermophy. Engg*. 3 (1999) 17-30.

[7] G. Maranzana, I. Perry, D. Maillet, Mini- and micro-channels: influence of axial conduction in the walls, *Int. J. Heat Mass Transf*. 47 (2004) 3993-4004.

[8] Z. Li, Y.L. He, G.H. Tang, W.Q. Tao, Experimental and numerical studies of liquid flow and heat transfer in microtubes, *Int. J. Heat Mass Transf*. 50 (2007) 3447-3460.

[9] S.X. Zhang, Y.L. He, G. Lauriat, W.Q. Tao, Numerical studies of simultaneously developing laminar flow and heat transfer in microtubes with thick wall and constant outside wall temperature, *Int. J. Heat Mass Transf*. 53 (2010) 3977-3989.

[10] M.K. Moharana, G. Agarwal, S. Khandekar, Axial conduction in single-phase simultaneously developing flow in a rectangular mini-channel array, *Int. J. Therm. Sci.* 50 (2011) 1001-1012.

[11] M. Karakaya, A.K. Avci, Microchannel reactor modelling for combustion driven reforming of iso-octane, *Int. J. Hydrogen Energy* 36 (2011) 6569-6577.

[12] R. Chein, Y.C. Chen, J.N. Chung, Axial heat conduction and heat supply effects on methanol-steam reforming performance in micro-scale reformers, *Int. J. Heat Mass Transf.* 55 (2012) 3029-3042.

[13] M.K. Moharana, P.K. Singh, S. Khandekar, Optimum Nusselt number for simultaneously developing internal flow under conjugate conditions in a square microchannel, *J. Heat Trans*., 134 (2012) 071703(01-10).

[14] M. Rahimi, R. Mehryar, Numerical study of axial heat conduction effects on the local Nusselt number at the entrance and ending regions of a circular microchannel, *Int. J. Therm. Sci.* 59 (2012) 87-94.

[15] G. Türkakar, T. Okutucu-Özyurt, Dimensional optimization of microchannel heat sinks with multiple heat sources, *Int. J. Therm. Sci*. 62 (2012) 85-92.

[16] D. Liu, S.V. Garimella, Analysis and optimization of the thermal performance of microchannel heat sinks, *Int. J. Numer. Methods Heat Fluid Flow* 15 (2005) 7-26.